Polarization Effects

W. G. Bagnuolo, Jr.
CHARA, Georgia State University, Atlanta, GA 30303

D.1. INTRODUCTION

This Appendix discusses the effects that polarization may have upon the visibilities measured by an interferometer, including errors caused by the varying intensities and, more importantly, phases of the seven telescope beams. Previous writers have studied these effects in long baseline interferometers; basic consensus is that they can be combatted successfully without a large additional system cost. The solution adopted by CHARA is first essentially to add two additional mirrors, so that the sequence of reflections of the beams from each telescope is the same. Secondly, we use a polarizing beamsplitter before final beam combination so that polarizations going to the imaging system from each beam are the same.

D.2. A POTENTIAL PROBLEM

In the original version of the design for the CHARA Array, the beams from the telescope "No. 5" mirror are directed down the light pipe toward the beam combining house. The geometries of the optical trains from the seven telescopes in the CHARA Array are thus identical except for two mirrors that translate the light from the telescopes to the central combining house. Therefore, even though the beams eventually have the same orientation, differences in polarization may result from the differences in reflectivity and phase delays of the beams. The problem is that the *sequence* of reflections is different for the three arms of the interferometer.

In an oblique reflection from a metallic surface, the electric vector of the incident light can be resolved into that in the plane of reflections (s) and that perpendicular to the plane (p). In general there will be an induced phase difference between the reflected p and s components.

Figure D.1 shows the relative delays between two linear polarizations along rays passing through the two relay mirrors for two telescope positions. (The two telescopes are assumed to be located along the $-x$ and $-y$ axes, respectively.) Consider the passage of light through the two mirrors at left. The polarization along the x–axis is denoted by a square indicating the beam orientation through the system. Because it is the p–polarization relative to the first mirror, this initial x–axis polarization suffers a delay of $-\Delta$ relative to the y–axis polarization, denoted by a short line segment. At the second mirror the x–polarization again acquires another delay, for a total phase of -2Δ relative to the y–polarization.

Tracing the ray from a telescope located in the $-y$ direction from the combining house, we see that the y–polarization this time is the p–polarization relative to both mirrors, and thus the x–polarization finishes with a total phase advance of $+2\Delta$ relative to the y–polarization. Furthermore, it is easy to see that for a case in which the telescope position is, say, at $(x, y) = (100,100)$, the two polarizations will strike both mirrors at 45° and no relative delay will result.

Figure D.2 shows the relative delays of the initial x–polarization. Because the CHARA

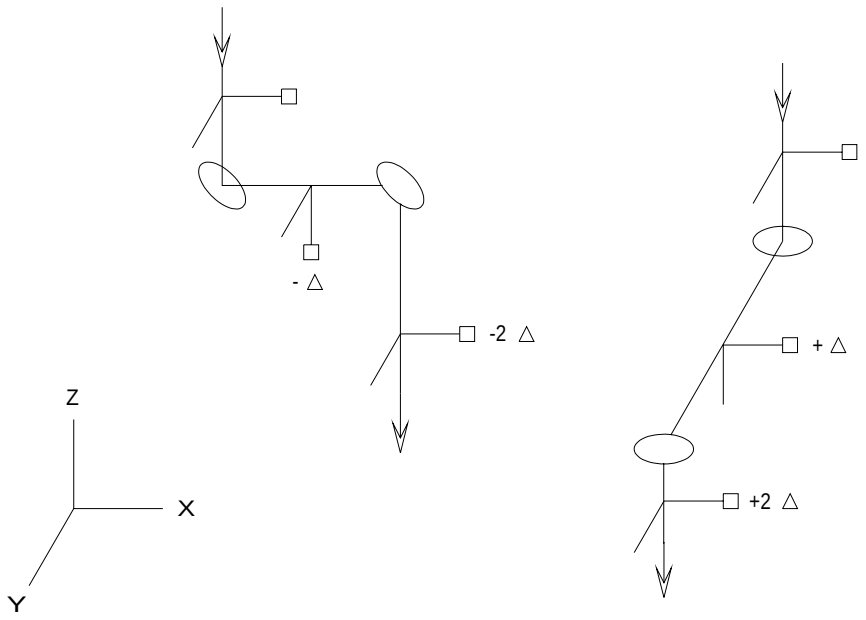

FIGURE D.1. Relative delay between two orthogonal polarizations caused by relay mirrors for two telescope locations.

Array will actually be in three arms of a Y separated by 120°, the worst case difference in delay between any two telescopes will be 3Δ, not 4Δ as in the example in Figure D.1. The implications of this phase shift will be discussed more fully later, but the potential problem involved can be seen from noting that at 550 nm, $\Delta \approx 26°$ for a silver mirror with an enhanced reflectivity coating (Traub 1988). A worst case phase difference of 78° could therefore have noticeable consequences in observed visibilities.

D.3. A SOLUTION

The most straightforward solution to the problem is simply to demand that the light from each telescope undergo the same sequence of reflections. Traub (1988) has shown an elaborate but elegant scheme for combining the light from three telescopes (see Figure D.3). Note that the light from each telescope is first relayed to the west, then is directed left, up, right, down, and right in Figure D.3. This type of rectilinear solution appears impractical for the CHARA Array because of both the distances involved and the much greater tube diameter. Figure D.4 shows an appropriate solution for the CHARA geometry which also has the advantage of using 30° angles of incidence instead of 45°, reducing the phase shift at each reflection by more than a factor of two according to Traub's data. This solution also only adds two additional reflections.

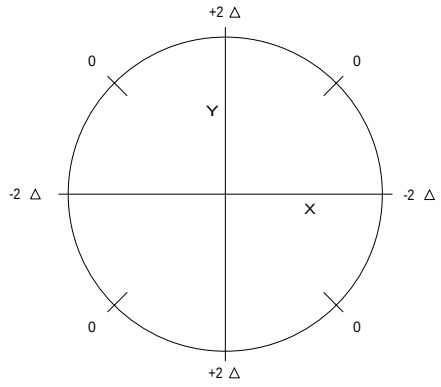

FIGURE D.2. Relative delays of initial x–polarization as a function of telescope location.

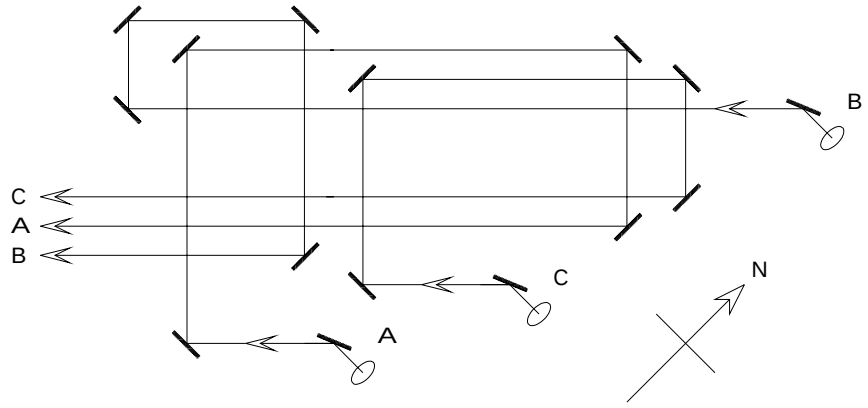

FIGURE D.3. Elimination of polarization effects of a three–telescope array by four 90° reflections. Light from telescopes A, B, and C are initially directed downward into the first mirrors shown.

D.4. A CALCULATION MODEL FOR POLARIZATION

In order to analyze the amount of polarization and the resulting optical delays in the optical train, the following analysis is presented. Most of the formalism for this analysis is taken from Borra (1976) and Shurcliff (1966). Borra's basic insight is that reflections off a metallic surface can be considered to be a combination of pure polarization and pure retardation. In matrix notation, the product of a polarization matrix (P) and a retardation plate (M) is calculated where the Mueller polarization representation is used. (More recently, Tango (1993) has used an alternative Jones Matrix approach.) Thus, for example, for the last three oblique reflections of a coudé system, the resultant polarization state J' is:

$$J' \;=\; P_5\; M_5\; P_4\; M_4\; P_3\; M_3\; J \tag{D.1}$$

where J equals the initial polarization state of the starlight, represented by the Stokes column vector $\{I, Q, U, V\} = \{1,\ 0,\ 0,\ 0\}$ for initially unpolarized light. Note that I is the intensity, and Q, U, V are the "horizontal preference", "plus 45° preference", and "right

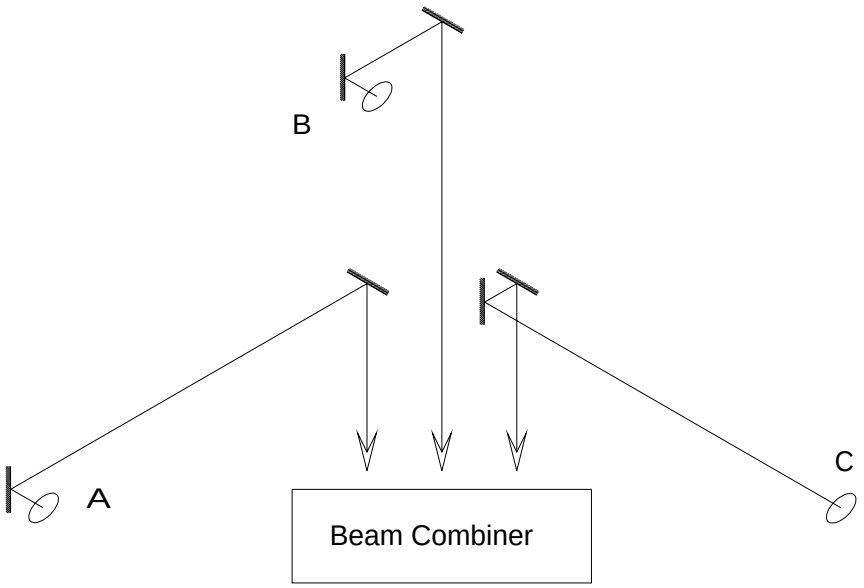

FIGURE D.4. Elimination of polarization effects in a CHARA–style array by two 60° reflections. Light from telescopes A, B, and C are initially directed downward as in Figure D.3.

circular preference", respectively.

According to Shurcliff and Borra the polarizer with the transmission axis "horizontal" can be written as:

$$P_0 \;=\; 0.5 \begin{pmatrix} k_s + k_p & k_s - k_p & 0 & 0 \\ k_s - k_p & k_s + k_p & 0 & 0 \\ 0 & 0 & 2\sqrt{k_s k_p} & 0 \\ 0 & 0 & 0 & 2\sqrt{k_s k_p} \end{pmatrix} \tag{D.2}$$

where k_s and k_p are the transmission coefficients ($k_s \equiv r_s^2,\ k_p \equiv r_p^2$).

For a general angle θ it can be shown that $P_\theta = T(\text{-}2\theta)\ P_0\ T(2\theta)$, where the "rotator matrix" is given by:

$$T(2\theta) \;=\; \begin{pmatrix} 1 & 0 & 0 & 0 \\ 0 & C_2 & S_2 & 0 \\ 0 & -S_2 & C_2 & 0 \\ 0 & 0 & 0 & 1 \end{pmatrix} \tag{D.3}$$

where $C_2 = \cos(2\theta)$ and $S_2 = \sin(2\theta)$.

The Mueller matrix for an ideal homogeneous retarder with retardance Δ and azimuth ρ measured from the fast axis is:

$$M(\rho) \;=\; \begin{pmatrix} 1 & 0 & 0 & 0 \\ 0 & D^2 - E^2 + G^2 & 2DE & -2EG \\ 0 & 2DE & -D^2 + E^2 + G^2 & 2DG \\ 0 & 2EF & -2DG & 2G^2 - 1 \end{pmatrix} \tag{D.4}$$

where $D \equiv \cos(2\rho)\,\sin(\Delta/2)$, $E \equiv \sin(2\rho)\,\sin(\Delta/2)$, and $G \equiv \cos(\Delta/2)$. Note that ρ is measured from the p direction and θ is measured from the s direction; thus at each mirror $\theta = \rho + 90^\circ$.

With these matrices the polarization effects can be calculated, provided that the geometry of the mirror train (θ's) and the coating properties (k_s, k_p, Δ) are known. Borra calculated the polarization effects of a five–mirror coudé system in which the contributions of the primary and secondary are neglected due to the almost normal incidence. In this system the fifth mirror directs the light horizontally to a coudé room. The principal direction chosen is contained in the plane of incidence of the light on mirror #5 (counted from the primary). This coudé system resembles a modified alt–az design.

Borra finds the following ρ angles for the last three mirrors of the coudé system: $\rho_5 = 0^\circ$ by definition, $\rho_4 = HA$, and $\rho_3 = HA - 90^\circ + \delta$, where HA and δ are the star's hour angle and declination.

For a similar modified alt–az system where mirror #5 directs the light southward, HA and δ are replaced respectively by $AZ + 90^\circ$ and AL, where AZ and AL are the azimuth and altitude of the star. Therefore, $\rho_5 = 0^\circ$, $\rho_4 = AZ + 90^\circ$, and $\rho_3 = AZ + AL$.

The locations of the telescopes relative to the central combining house have azimuths of $TA \equiv 0^\circ$, 120°, or 240° for the north, east, or west arms of the array, where TA denotes telescope azimuth. Mirror #7 directs the light southward into the combining house, and its "fast axis", horizontal to the ground, can be designated as $\rho_7 \equiv 0^\circ$. The two relay mirrors, numbers 5 and 6, have axes at $\rho_5 = \rho_6 = TA$ relative to mirror #7. The ρ angles of all mirrors prior to mirror #5, relative to this mirror, were given above. Thus, $\rho_7 = 0^\circ$, $\rho_6 = \rho_5 = TA$, $\rho_4 = TA + AZ + 90^\circ$, and $\rho_3 = TA + AZ + AL$. With these geometric parameters being so defined, the polarization effects of the first six mirrors can be calculated. Note that at mirror number 7 and beyond, the light paths are identical for all telescopes. The material properties assumed for the enhanced reflectivity coatings, based on those given by Traub (1988), are: $k_s = 0.99$, $k_p = 0.97$, and $\Delta = 28^\circ$ at 506 nm.

A first test is obtained by assuming initially unpolarized light and computing the relative intensity of the output light polarized parallel to $\rho = 0^\circ$ at the seventh mirror. The average intensity throughput efficiency was 0.922. The maximum differential change in intensity is 4.7% for $AL = 90^\circ$, $AZ = 120^\circ$, and $TA = 0^\circ$ and 240°. Table D.1 lists these results. It appears that for unpolarized sources the induced polarization produces relatively small effects on intensities (and visibilities if these effects are not corrected). Still, the beam intensities in the polarization(s) used must be calibrated before being combined.

A second test assumes that light is initially in the state {1,1,0,0}, *i.e.* linearly (horizontally) polarized. Table D.2 shows the intensity output relative to a purely horizontally polarized output with 0.922 intensity (the average overall transmission). Note that in the extreme cases, the intensity is reduced to about 45% of the input level. The worst difference between the three telescope azimuths occurs at $(AL, AZ) = (60^\circ, 120^\circ)$, where the relative intensities are 0.922, 0.451, and 0.721, respectively, The conclusion from these data is that a highly polarized source will experience large induced changes in intensity with the "baseline" design for the CHARA Array. On the other hand, visual sources with polarizations of more than

TABLE D.1. Intensity changes in initially unpolarized light.

AL	*AZ*	Telescope Azimuth (0°)	(120°)	(240°)
90°	0°	0.000	-0.003	-0.003
	30°	-0.014	0.021	-0.008
	60°	-0.026	0.021	0.009
	90°	-0.041	0.000	0.000
	120°	-0.026	0.009	0.021
	150°	-0.014	-0.008	0.021
60°	0°	-0.007	-0.008	0.008
	30°	-0.015	0.011	-0.008
	60°	-0.021	0.023	0.002
	90°	-0.034	0.009	0.004
	120°	-0.033	0.001	0.010
	150°	-0.018	-0.008	0.024
30°	0°	-0.014	-0.001	0.011
	30°	-0.010	0.004	0.003
	60°	-0.016	0.012	-0.001
	90°	-0.025	0.012	0.002
	120°	-0.031	0.009	0.009
	150°	-0.025	0.000	0.013

a few percent are rare, and extra compensation could be used for such sources. However, Borra points out that compensation using, for example, a Babinet–Soleil compensator is only partial.

A final effect of polarization is that the phase delay Δ is actually a function of the wavelength. Traub has found that between 506 and 604 nm, Δ declines from 28° to 24°. Thus the 3Δ maximum difference discussed in Section D.2 would vary by only about 12° even over a bandwidth this wide. Therefore, this effect is insignificant.

D.5. CONCLUSIONS

Polarization effects with the baseline design of the CHARA Array are not very large for unpolarized sources, but they must still be considered in the analysis of such data. For partially polarized sources, such as resolved hot star photospheres, where electron scattering is a significant source of opacity, the induced polarization effects could be severe if uncorrected. A design like that of Figure D.3 involves somewhat greater mechanical complexity while saving marginally on mirror costs due to the downsized flats. (The steeper angles of incidence permit the use of potentially smaller diameter flats than for 45° incidence angles.) We decided to adopt the two additional mirrors of Figure D.3 to eliminate a known polarization problem. As an additional precaution, we have used a polarizing beam-splitter to separate the light going into the imaging/tilt systems from that going to the fringe-tracker. This method has been used successfully on the SUSI Array (Tango 1993). Our current (revised) design could also permit the observation of interesting polarized objects at high resolution.

TABLE D.2. Relative intensity (initial linear polarization).

AL	*AZ*	Telescope Azimuth (0°)	(120°)	(240°)
90°	0°	1.000	0.997	0.997
	30°	0.825	0.985	0.825
	60°	0.810	0.860	0.451
	90°	0.960	0.489	0.489
	120°	0.810	0.451	0.860
	150°	0.825	0.825	0.985
60°	0°	0.951	0.950	1.005
	30°	0.951	0.991	0.940
	60°	0.815	0.929	0.652
	90°	0.923	0.679	0.469
	120°	0.922	0.451	0.721
	150°	0.816	0.661	0.971
30°	0°	0.942	0.832	0.969
	30°	0.988	0.952	0.960
	60°	0.942	0.944	0.832
	90°	0.932	0.832	0.665
	120°	0.967	0.665	0.691
	150°	0.932	0.657	0.867

D.6. REFERENCES

Borra, E.F., 1976, *PASP*, **88**, 548
Shurcliff, W.A., 1966, *Polarized Light*, (Cambridge: Harvard Univ. Press)
Tango, W.J., 1993, private communication
Traub, W.A., 1988, "Polarization Effects in Stellar Interferometers" in *High–Resolution Imaging by Interferometry*, ESO Conference Proc. No. 29, 1029
Walker, G., 1987, *Astronomical Observatories*, (Cambridge: Cambridge Univ. Press), 113